

Supplemental Figure Legends

Supplemental Figure 1 (in reference to Figure 2)

(A) Aggregate flow cytometric data of IL-4-stimulated BMDMs showing CD206⁺/CD71⁺ treated with increasing concentrations of etomoxir for 24 hr. Values given are the geometric mean of fluorescence intensity. (n = 6 independent biological replicates)

(B) Flow cytometric analysis of CD301 expression in response to low (3 μ M) or high (200 μ M) etomoxir. The data shown are from one experiment representative of a total of six independent biological replicates.

(C) Measurements of arginase activity in BMDMs with IL-4 \pm 200 μ M etomoxir co-treatment for 24 hr. Data represents two independent biological replicates.

(D) (Left) qPCR analysis on the expression of *Cpt1a*, *Cpt1b*, and *Cpt1c* in WT and *Cpt1a*^{-/-} BMDMs co-treated with IL-4 \pm etomoxir for 24 hr. Data represent two independent replicates. (Right) Quantification of CPT1a protein levels in WT or *Cpt1*^{-/-} peritoneal macrophages. Each lane represents one individual mouse.

(E) Representative data from an individual experiment measuring uncoupler-stimulated respiration \pm 3 μ M etomoxir in permeabilized WT or LysM-Cre *Cpt1*^{-/-}. BMDMs were offered either palmitoyl CoA/malate/carnitine or palmitoylcarnitine/malate as substrates to measure respiration specifically mediated by CPT-1 activity. (n = 5 technical replicates from a single biological replicate). BMDMs were treated with IL-4 for 24 hr. prior to measurements.

(F) Etomoxir-sensitive respiration was defined as the difference in FCCP-simulated respiration rates \pm 3 μ M etomoxir. (n = 4 independent biological replicates). *Cpt2*^{-/-} BMDMs were offered pyruvate, rather than palmitoylcarnitine, because CPT-2 is required for oxidation of both palmitoyl CoA as well as palmitoylcarnitine.

(G) Flow cytometric analysis for CD206⁺/CD71⁺ in WT and *Cpt2*^{-/-} BMDMs differentiated with IL-4 \pm 3 μ M or 200 μ M etomoxir. The data shown are from one experiment

representative of a total of three independent biological replicates.

(H) Flow cytometric analysis for the CD206⁺/CD71⁺ population in WT and *Cpt1a*^{-/-} BMDMs differentiated with IL-4 ± 3 μM or 200 μM etomoxir. The data shown are from one experiment representative of a total of three independent biological replicates.

(I) Lactate effluxed to the experimental medium by WT, *Cpt1*^{-/-}, and *Cpt2*^{-/-} BMDMs in response to 24 hr treatment with IL-4. Cells were offered 8 mM glucose, 2 mM glutamine, and 2 mM pyruvate. (n = 3 independent biological replicates)

Supplemental Figure 2 (in reference to Figure 3)

(A) Maximal FCCP-stimulated respiration in response to 3 μM etomoxir in six cell types (experimental conditions in Materials and Methods). As positive controls, all cell types showed sensitivity to either the glutaminase inhibitor BPTES or the mitochondrial pyruvate carrier inhibitor UK5099 (both at 3 μM). (n ≥ 3 independent biological replicates)

(B) (Left) Maximal respiration in HepG2 cells offered 8 mM glucose, 2 mM glutamine, and 2 mM pyruvate in the experimental medium with BPTES and UK5099 (both at 3 μM) ± 3 μM etomoxir. (n = 4 independent biological replicates). (Right) Maximal respiration in 3T3-L1 adipocytes offered 1 mM glucose and 0.5 mM carnitine in the experimental medium with increasing concentrations of etomoxir. (n = 3 independent biological replicates)

(C) Sample respirometry trace of A549 cells offered 8mM glucose, 2 mM glutamine, and 2 mM pyruvate in the experimental medium ± 100 μM etomoxir. (n = 5 technical replicates)

(D) Sample concentration-response curve of ATP-linked and maximal FCCP-stimulated respiration in A549 cells [conditions as in (A & C)] in response to increasing concentrations of etomoxir. (n = 5 technical replicates)

(E) Aggregate EC₅₀ values for the inhibition of ATP-linked and maximal FCCP-stimulated

respiration by etomoxir in a range of intact cells. Experimental conditions are as in (A) and available in Materials and Methods. ($n \geq 3$ independent biological replicates)

Supplemental Figure 3 (in reference to Figure 3)

(A) Sample respirometry trace of permeabilized HepG2 cells offered pyruvate/malate and either 30 μM or 300 μM of etomoxir. ($n = 5$ technical replicates)

(B) Aggregate EC_{50} values for the inhibition of ATP-linked and maximal FCCP-stimulated respiration by etomoxir in permeabilized HepG2 or A549 cells. Pyr, cells offered pyruvate/malate as respiratory substrates; Glu, glutamate/malate; Gln, glutamine (no malate required). ($n = 4$ independent biological replicates)

(C) Phosphate-induced swelling assay in isolated rat liver mitochondria. Loss of absorbance reflects mitochondrial swelling due to activity of the P_i carrier (see Materials and Methods). Etomoxir does not affect the rate of swelling as there was no change in loss of absorbance relative to the control. As expected, inhibitors of mitochondrial carriers including N-ethyl maleimide (NEM) and mersalyl both inhibited the rate of swelling. As a positive control for rapid and complete loss of absorbance, 10 $\mu\text{g}/\text{mL}$ alamethicin (Alm) was used to permeabilize the inner membrane to small solutes and induce osmotic swelling.

(D) Scheme depicting how ATP hydrolysis can be measured by pH changes in the experimental medium. Phosphorylating respiration will alkalinize the experimental medium (*top*), and ATP hydrolysis by the ATP synthase will acidify the experimental medium (Divakaruni et al., 2017a). IMS, intermembrane space; MIM, mitochondrial inner membrane.

(E) A sample kinetic trace using isolated rat liver mitochondria showing pH changes in the experimental medium in response to ATP synthesis or hydrolysis by the ATP synthase. P/M/ADP, pyruvate/malate/ADP; rot/antiA, 2 μM rotenone/1 μM antimycin A.; FCCP/ATP, 1 μM FCCP and 25 mM ATP; CAT, 5 $\mu\text{g}/\text{mg}$ mito. protein

carboxyatractyloside. (n = 10 technical replicates)

(F) Effects of 100 μ M etomoxir in “double-permeabilized” HepG2 cells (Divakaruni et al., 2017a). In the presence of both rPFO (plasma membrane permeabilization) and 10 μ g/mL alamethicin (mitochondrial membrane permeabilization), NADH and succinate can reach the matrix side of the inner membrane unimpeded, allowing, respectively, direct measurement of complex I- and complex II-mediated respiration. [NADH], 2 mM; [succinate], 5 mM. Both NADH (2 mM) and succinate (5 mM) were added in the presence of 10 μ M cytochrome c. (n = 4 independent biological experiments)

(G) ADP-stimulated (State 3) or maximal FCCP-stimulated respiration was measured in permeabilized WT, *Cpt1a*^{-/-}, and *Cpt2*^{-/-} BMDMs \pm 200 μ M etomoxir. Permeabilized cells were offered pyruvate/malate as respiratory substrates. (n = 4 independent biological replicates)

Supplemental Figure 4 (in reference to Figure 3)

(A) Basal mitochondrial respiration in intact BMDMs after 24 hr treatment with 100 nM piericidin A (PierA). (n = 4 independent biological replicates)

(B) Measurement of β -oxidation in IL-4-stimulated BMDMs treated with etomoxir (either 3 or 200 μ M), rotenone (200 nM) or antimycin A (200 nM). Data represents three independent experiments.

(C) Normalized cell counts from Seahorse XF96 plates for WT BMDM stimulated with IL-4 and co-treated with 200 μ M etomoxir (Eto), 200 nM rotenone (Rot), 200 nM antimycin A (AntiA), 1.2 μ M oligomycin (Oligo), or 5 μ M carboxyatractyloside (CAT) for 24 hr.

(D) Flow cytometric analysis for CD206, CD71, and CD301 in BMDMs stimulated with IL-4 \pm 200 nM rotenone or 100 nM piericidin A (PierA, co-treated with IL-4) for 48 hr. The data shown are from one experiment representative of a total of four independent biological replicates.

(E) qPCR analysis of *Relma*, *Mgl2*, *Ym1*, *Fabp4*, and *Arg1* after 24 hr treatment of IL-4 \pm

100 nM piericidin A for 24 hr. (n = 3 independent biological experiment)

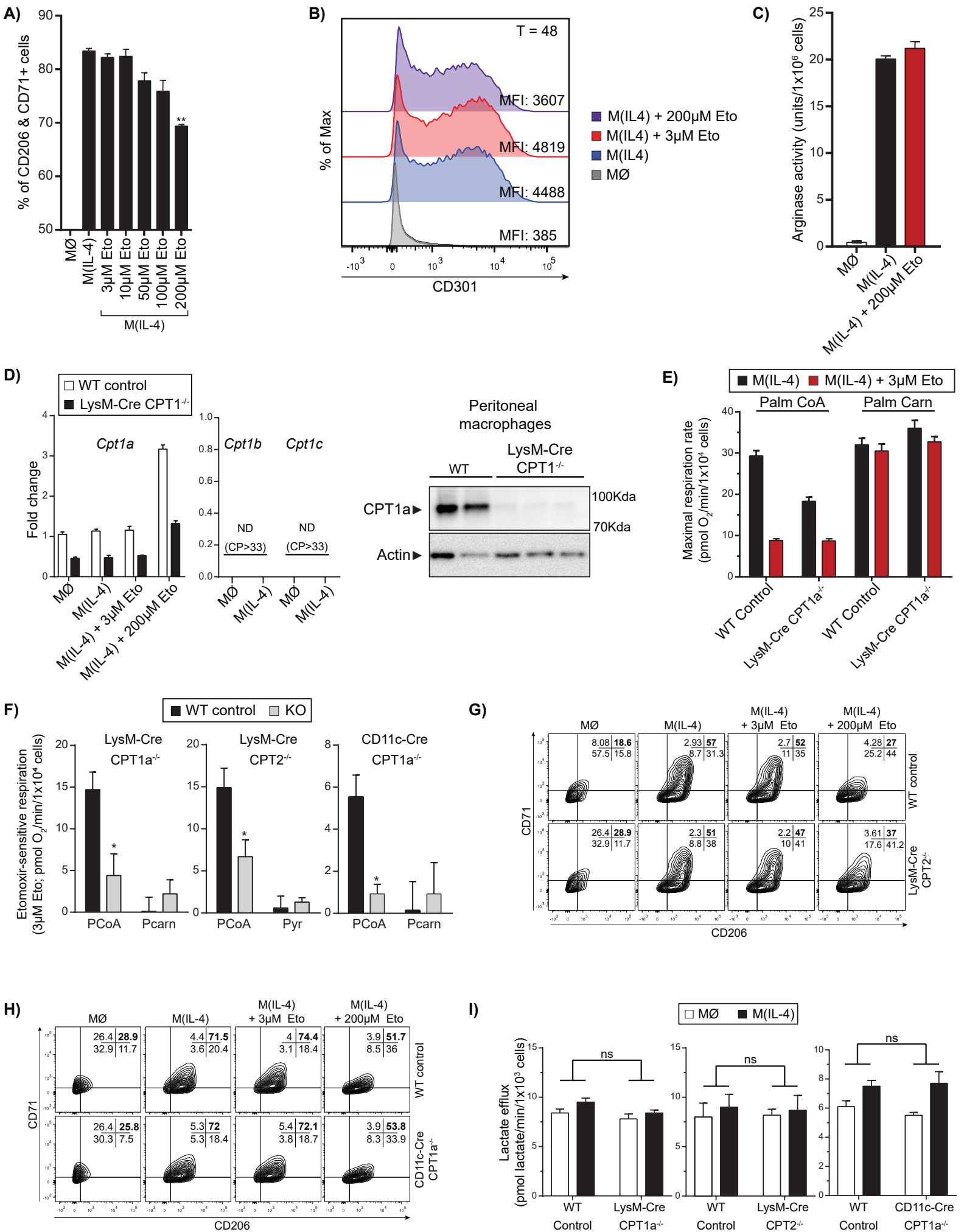
Supplemental Figure 5 (in reference to Figures 4 and 5)

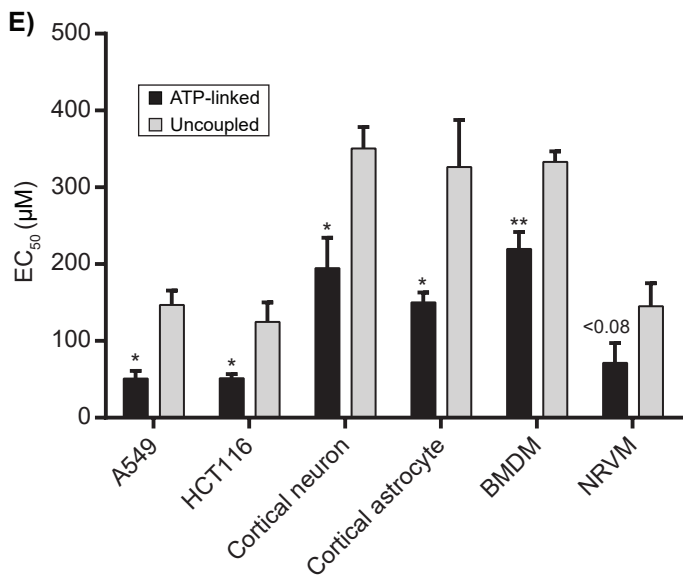
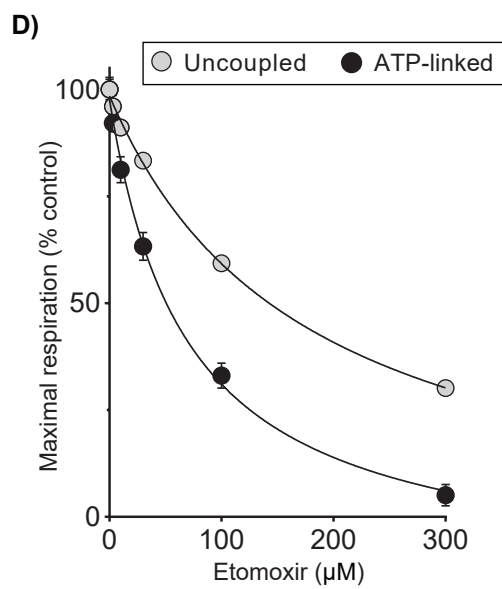
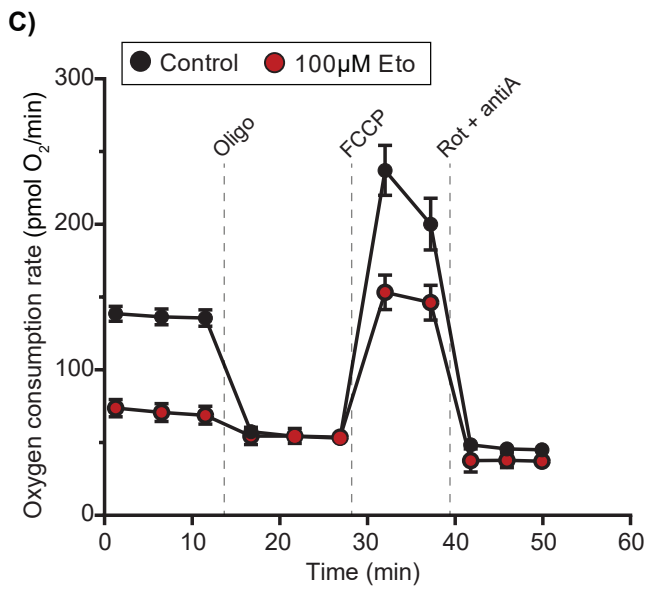
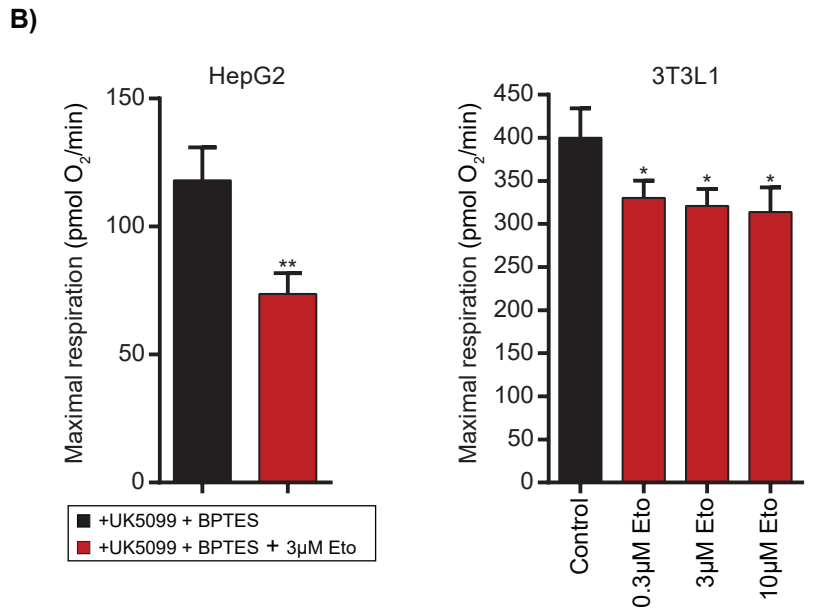
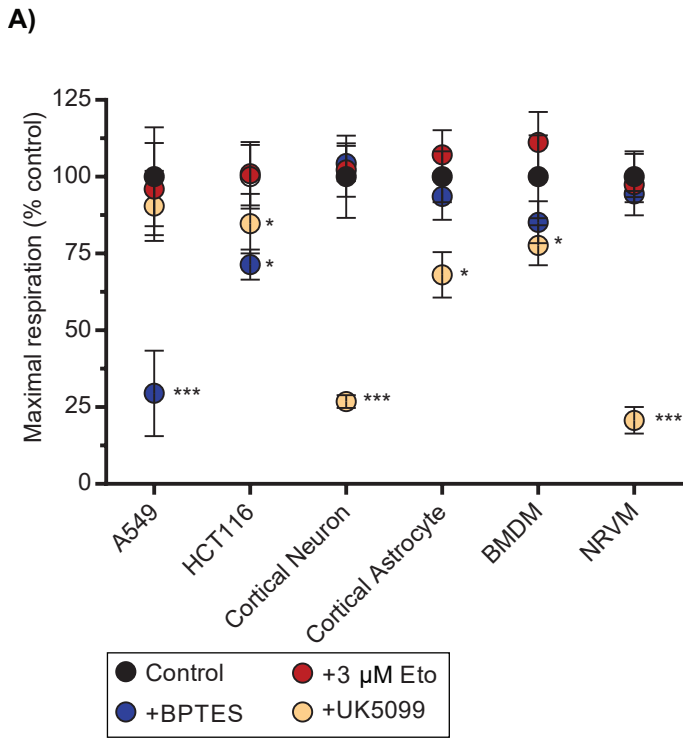
(A) Heat map of LC-MS metabolomics data showing the 70 metabolites with an ANOVA p-value ≤ 0.05 from WT BMDM, 24 hr. IL-4 stimulation, IL-4 + 3 μM etomoxir, and IL-4 + 200 μM etomoxir. Cells were co-treated with IL-4 and etomoxir. Data are from three technical replicates. Bar reflects scaled relative amounts of metabolites across conditions.

(B) Basal mitochondrial respiration in intact BMDMs after 24 hr treatment with IL-4 \pm 500 μM CoA. (n = 4 independent biological replicates)

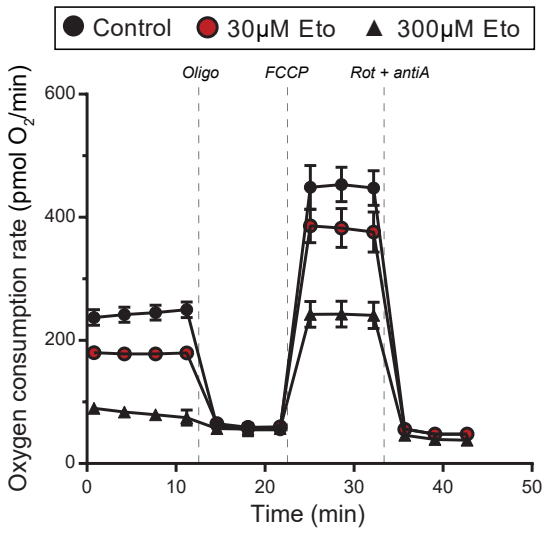
(C) Flow cytometric analysis of the CD206⁺/CD71⁺ population in WT and *Cpt2*^{-/-} BMDMs in response to IL-4 \pm 200 μM etomoxir \pm 500 μM CoA. The data shown are from one experiment representative of a total of three independent biological replicates.

(D) Flow cytometric analysis of the CD206⁺/CD71⁺ population in WT and CD11c-Cre *Cpt1*^{-/-} BMDMs in response to IL-4 \pm 200 μM etomoxir \pm 500 μM CoA. The data shown are from one experiment representative of a total of two independent biological replicates.

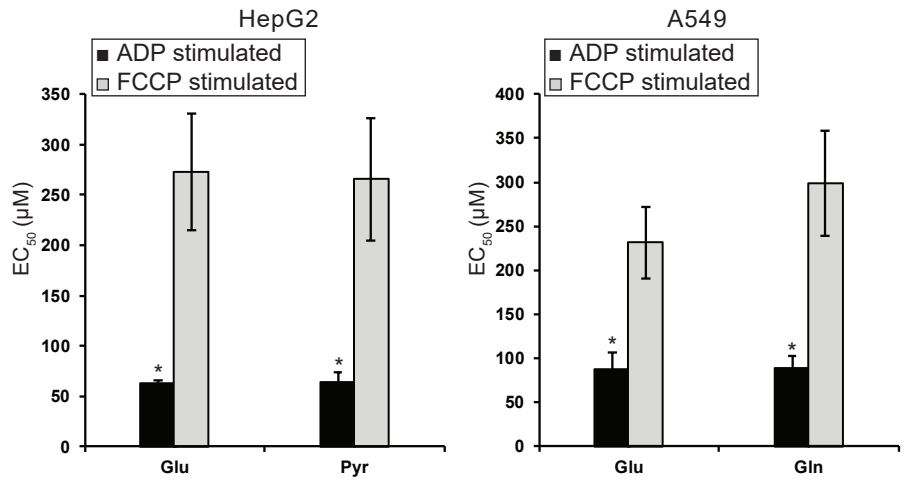




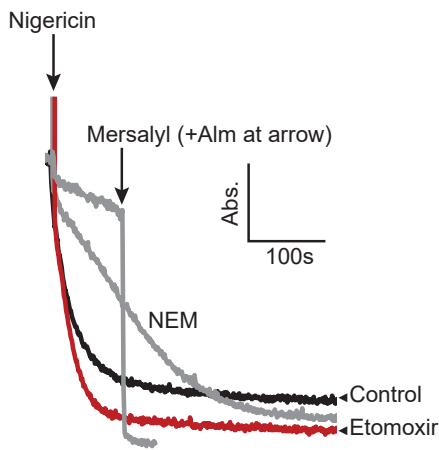
A)



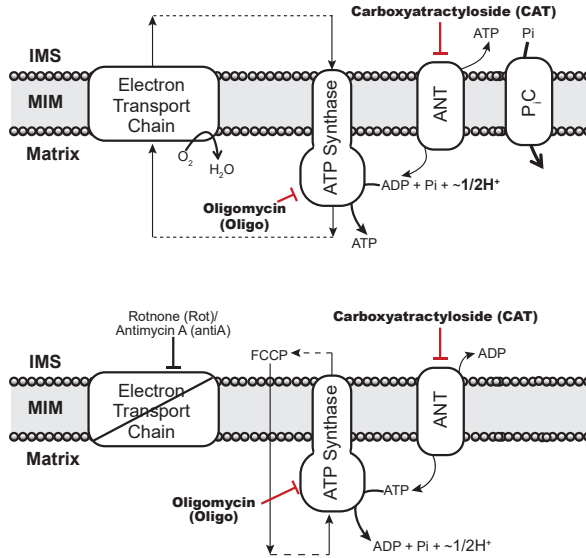
B)



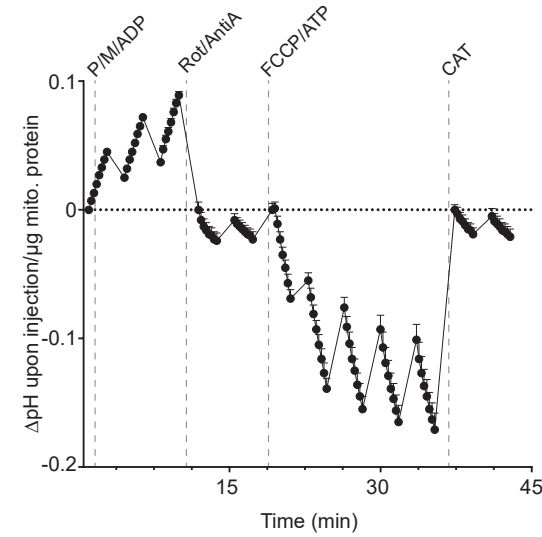
C)



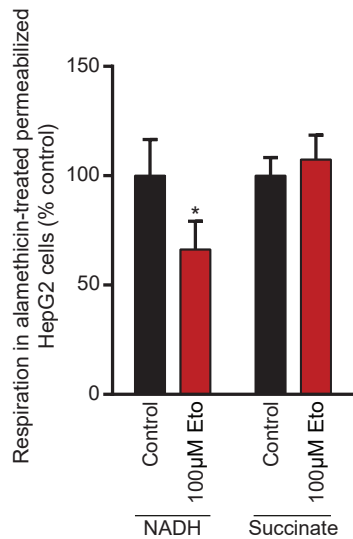
D)



E)



F)



G)

